Artigo Original

Revista Brasileira de Física Médica (2020) 14:534

CBCT Image Registration for Adaptive Radio and Proton Therapy of Prostate Cancer

Fusão de Imagens de CBCT para Radioterapia e Protonterapia Adaptativa de Câncer de próstata

Roberto Cassetta[1], Marco Riboldi[2], Kleber Leandro[3], Marco Schwarz[4], Vinicius Gonçalves[5], Paulo Eduardo Novaes[3], Roberto Sakuraba[5], Roger Guimaraes[3], Guido Baroni[1]

1.DEIB, Politecnico di Milano, Milan, Italy
2.Faculty of Physics, Ludwig-Maximilians-Universität (LMU), Munich, Germany
3.Radiotherapy Department, Hospital Vitoria, Santos, Brazil
4.Proton therapy Department, Trento Hospital, Trento, Italy
5.Radiotherapy Department, Hospital Israelita Albert Einstein, Sao Paulo, Brazil

Abstract

The application of cone-beam CT (CBCT) image guidance in external beam therapy for prostate cancer treatment is questioned by sub-optimal image quality and procedural constraints. Such factors may frustrate the effort of applying volumetric imaging to quantify anatomical changes and evaluate replanning. This study investigates the impact of anatomical changes and the potential of using CBCT for IMRT and IMPT in prostate patients. Deformable image registration (DIR) is applied in 9 prostate cancer patients imaged with CBCT, to transform the planning CT and produce a virtual CT with updated patient anatomy. Daily image guidance was simulated for repeated CBCT scans relying on either soft tissue targeting or bone anatomy matching. Automated landmark detection was used to evaluate the residual distance for landmarks distributed over the region of interest (target and organs-at-risk) after DIR. DIR allowed the mean distance for these landmarks to be reduced from 3.79 to 2.00 mm. IMRT and IMPT plans were created and recalculated over virtual CTs. Rectum dose increase was observed in 8 of 9 patients, and for 3 cases there was constraints violation, accordingly to QUANTEC guidelines, of up to 75 Gy on 19% of rectum volume. The most important CTV coverage loss was around 5% of the prescribed dose for a proton therapy case. For both types of treatment, PTV inter-fraction movement and organs-at-risk structural variations, may result in loss of target coverage and/or early excessive damage of acute-responding tissue components. Therefore, DIR and dose recalculation are important tools for dose distribution verification on PTV and organs at risk, in order to assure prescribed dose delivery and avoid future complications.

Keywords: CBCT; image registration; adaptive radiotherapy.

Resumo

O uso de CBCT na radioterapia para o tratamento do câncer de próstata é questionada por restrições de qualidade de imagem e limitações técnicas. Tais fatores podem frustrar o intento de utilizar imagens volumétricas para quantificar as alterações anatômicas e avaliar o plano de tratamento. Este estudo investiga o impacto de alterações anatômicas e o potencial do uso de CBCT para IMRT e IMPT em pacientes de câncer de próstata. A fusão deformável (DIR) de imagens é aplicada em 9 pacientes com câncer de próstata escaneados com CBCT, para adaptar a tomografia de planejamento e produzir uma tomografia virtual com anatomia atualizada do paciente. O acompanhamento diário por imagem foi simulado com CBCT repetidas, com base nos tecidos moles ou na correspondência da anatomia óssea. A detecção automática de pontos de referência foi usada para avaliar a distância residual dos pontos de referência distribuídos na região de interesse (alvo e órgãos em risco) após o DIR. O DIR permitiu que a distância média desses marcos fosse reduzida de 3.79 para 2.00 mm. Os planos IMRT e IMPT foram criados e recalculados em tomografias virtuais. O aumento da dose do reto foi observado em 8 dos 9 pacientes, e em 3 casos houve violação das restrições, de acordo com as diretrizes do QUANTEC, de até 75 Gy em 19% do volume do reto. A perda de cobertura de CTV mais importante foi em torno de 5% da dose prescrita para um caso de terapia de prótons. Para ambos os tipos de tratamento, o movimento inter-fração de PTV e variações estruturais de órgãos em risco, podem resultar em perda de cobertura de alvo e / ou dano excessivo precoce em tecido de resposta aguda. Portanto, o DIR e o recálculo da dose são ferramentas importantes para a verificação da distribuição da dose no PTV e nos órgãos de risco, a fim de garantir a entrega da dose prescrita e evitar complicações futuras.

***Palavras-chave**: CBCT; fusão de imagens; radioterapia adaptativa.*

1. Introduction

Image guided radiotherapy entails frequent imaging during treatment to enhance the accuracy in treatment delivery. The imaging workflow provides the ability to check changes occurring over the course of therapy, thus offering the potential for treatment adaptation (adaptive radiotherapy -ART). Cone-beam CT (CBCT) imaging has found widespread clinical

application in recent years, in order to quantify volumetric changes which might influence CTV coverage and critical organ sparing (1). Although it features worse image quality than CT, CBCT provides volumetric imaging on the treatment couch. This benefit can be exploited to update the treatment plan (2), following the ART concept (3). The basic requirement to implement ART is the ability to quantify the actually delivered dose in changing anatomy ("dose of the day" calculation), as a way to evaluate the need of a new CT image acquisition for treatment re-planning purposes (4,5). Similar concepts can be potentially applied to proton therapy as well; at the current status, the implementation of treatment adaptation protocols is restrained by the reduced availability of volumetric imaging devices in proton therapy facilities (6).

Deformable Image Registration (DIR) applies a non-rigid transformation to the planning CT, in order to model any intra-fractional geometric change in patient's anatomy, which enables daily dose recalculation and the evaluation of re-planning needs. Head and neck (H&N) and prostate cases have been studied and considered for the implementation of DIR using CBCT images. Recent works in the H&N and prostate region show that deformable registration relying on CBCT-CT information could be useful for daily dose recalculation and dose accumulation analysis (7–10).

Treatment options for prostate cancer irradiation include both conventional X-ray radiotherapy and proton therapy. Radiotherapy with proton beams has brought promising results when compared to conventional photons treatment (11–13), especially for sparing critical structures adjacent to the tumor (14,15). To fully exploit the potential of proton therapy, millimetric precision is required to avoid under- or over-shooting, which could drastically affect clinical outcomes. To consider uncertainties of the Bragg peak position regarding anatomy changes (16) and its dependency on the CT-based stopping power remapping, repeated CT scans are required resulting, at least, in more dose delivered to the patient and elevation of time and costs to complete the treatment. DIR based on volumetric CBCT scans is a potential alternative to such an issue, by producing deformed CTs based on the actual patient anatomy depicted in CBCT images.

The application of CBCT-CT DIR to prostate cases is extremely challenging for the following reasons:

- Reduced field-of-view (FOV) CBCT might not include all the patient tissues traversed by the therapeutic beam, thus limiting the estimation of beam interaction with the new anatomy. This applies also to proton therapy, as large FOV CBCT are not yet always available clinically.

- CBCT image quality in the pelvic region is a critical issue, due to the suboptimal image contrast in X-ray projections and to the significant scatter-to-primary ratio (SPR). Image quality is therefore expected to affect the performance of CBCT-CT DIR.

- Large localized deformation for organs at risk around the prostate, like bladder and rectum, which is difficult to recover and might present large inter and intra fraction variability (17–20).

- Patient positioning takes a considerable time regarding the whole daily fraction delivery, as reproducibility in the pelvis region is hard to achieve(21). Including acquisition of volumetric images and using them to estimate the occurred deformation (vector field) can be time consuming.

In this study, we present a CT to CBCT deformable registration method based on the ITK library (22). An algorithm was developed to explore the soft tissue information of the CT-CBCT images to perform deformable registration, making efforts to overcome the poor signal-to-noise ratio that limits CBCT use for treatment planning purposes. This study evaluates the potential of using large FOV CBCT for IMRT and IMPT prostate patients, due to the evidence of positives outcomes from the treatment with protons (23,24). As the prostate could move or present deformations independently of the surroundings bone structure, taking into account soft tissue information could lead to a more precise treatment, since pelvic bone-based alignments may underdose the prostate in one-third of the fractions (25). We specifically evaluate dosimetric results in 9 prostate cases undergoing repeated CBCT imaging, evaluating the sensitivity of IMRT and IMPT treatment plans to anatomical changes. These analyses were based on QUANTEC (Quantitative Analysis of Normal Tissue Effects in the Clinic) guidelines, which summarize the dose/volume tolerance recommendations for treatment planning(26). To complement our visual assessment of performance, we use the Scale Invariant Feature Transform (SIFT)(27,28). SIFT has shown itself to be an useful tool for DIR evaluation, as an automated way to find matching features between images and measure their residual distances following DIR application(29). This study aims at DIR based on large FOV CBCT investigation as a clinical tool for radio and proton therapy of prostate cancer patients.

2. Materials and methods

2.1 Patient Data

The planning CT from 9 patients and CBCT images acquired over the treatment course (28 in total) were selected from Hospital Albert Einstein (SP-Brazil) database. The CT images were obtained with GE light speed multi slice, whereas CBCT images with Varian 23EX, both featuring a voxel size of 1.39, 1.39, 2.5 mm along RL, CC and AP directions, respectively. The PTV was defined with a 10 mm margin in anterior and lateral directions, and 7 mm expansion in the posterior direction with respect to the CTV. Patients were instructed to drink 500 ml of water 45 minutes before treatment and to follow a specific diet in order to avoid unintended increase in the rectum volume. The CBCT images were acquired within a month from the CT acquisition date.

2.2 Deformable image registration

A C++ code based on the ITK Library was developed to create a method for deformable registration between CT-CBCT images of the same patient. The Insight Segmentation and Registration Toolkit (ITK) is an open-source project that provides an extensive list of tools for image analysis and allows one to develop algorithms for clinical research.

The first steps of the algorithm were as follows: (i) rescaling the intensity of the CBCT image and (ii) applying a histogram-matching filter between both images, which also facilitates feature extraction (see section 2.3). The selected metric was Mattes Mutual Information(30), largely used for multi-modality images(22). As optimizer, we used the limited-memory Broyden–Fletcher–Goldfarb–Shanno (L-BFGSBO). To handle the deformable transformation between the two images, we configured the B-Spline interpolator in our algorithm. An example of DIR results can be seen in figure 1. Hereafter, we call $_{v}$CT (virtual CT) the deformed $_{p}$CT (planning CT), i.e., the product of the DIR between $_{p}$CT and CBCT. The virtual CT is meant to represent a CT image matching the anatomical features observed in the CBCT acquired during treatment.*2.3 Scale Invariant Feature Transform (SIFT) for DIR validation*

We used the n-dimensional scale invariant feature transform method to automatically extract and match features from each pair of CT and CBCT images. SIFT allows the assessment of image registration results through residual errors evaluation at corresponding landmarks (8,29,31). Number and location of landmarks are strictly dependent on the settings applied for the SIFT descriptor, and on local contrast in the considered image dataset. After finding correspondent points between the CBCT and the transformed CT, outliers were discarded, then, the distance of each landmark pair was measured, thus providing the quantification of residual errors for each anatomical direction. The inverted vector field found during DIR was applied to matching points to measure their initial position at the planning CT and quantify the similarity improvement through image registration. A paired two-sided sign test was applied to verify statistically significant differences between initial and residuals landmark differences, at 99% statistical confidence. For the 9 patients, a delimited ROI (PTV+OAR) was used for SIFT measurements. The landmarks obtained by SIFT feature extraction were distributed among soft and rigid tissue, according to local contrast in the selected ROI (figure 2). Around 200 correspondent points were found for each pair of images ($_{v}$CT-CBCT).

2.4 Planning CT Warping

The vector fields obtained from the deformed registration were applied to the planning CTs and contours with the function warp of PLASTIMATCH (32). This procedure allowed the creation of a $_{v}$CT with new contours, representing updated patient anatomy.

2.5 Treatment planning and recalculation

We used 5-field IMRT plans for Photons and 2 contralateral treatment fields IMPT plans for protons (figure 3). The dose prescription was 76 Gy in 2 Gy per fraction.

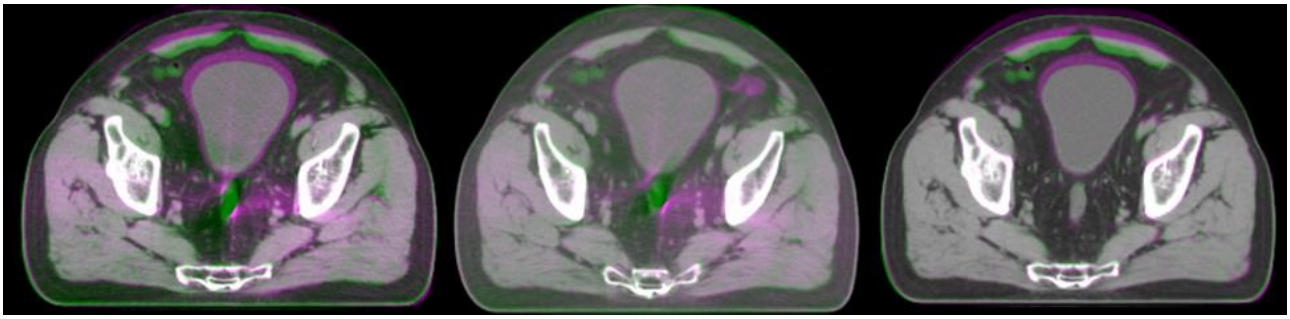

Figure 1: Comparison among: $_{p}$CT-CBCT (left), $_{v}$CT-CBCT (middle) and $_{v}$CT-$_{p}$CT (right).

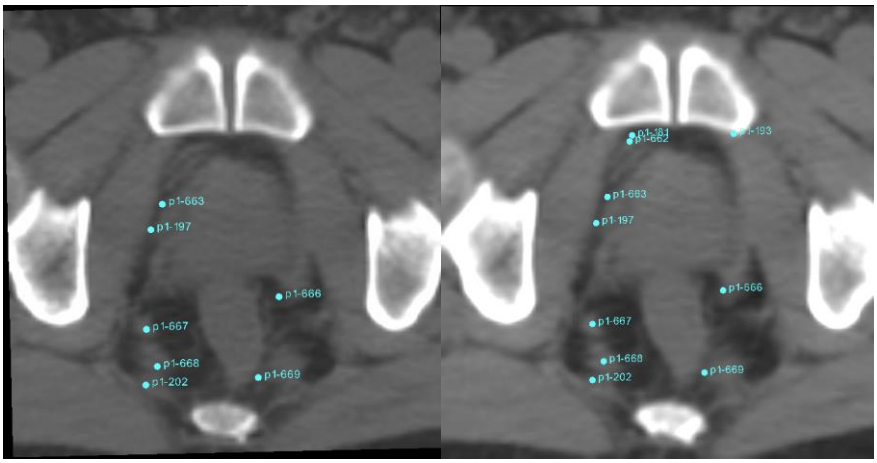

Figure 2: Automatic SIFT landmarks extracted before DIR (left) and after DIR (right). The displacement of landmarks is observed on axial plane or their disappearance when moving on cranio-caudal direction.

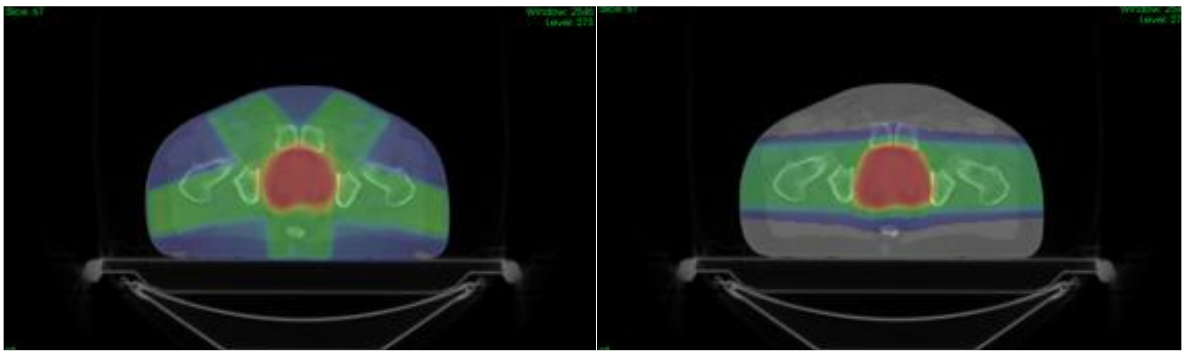

Figure 3: IMRT plan (left), IMPT plan (right).

The original plan was applied to the warped CTs to verify the delivered dose distribution in the deformed anatomy. For photons, the Eclipse (Varian Medical Systems – Palo Alto, CA) treatment planning software was used for IMRT planning and dose recalculation. For protons, RayStation6 (RaySearch Laboratories) was used for IMPT planning and quantification of dose in deformed anatomy.

Before IMRT dose recalculation, images were rigidly registered in the treatment planning system (TPS) based on the PTV region, mimicking CBCT-guided inter-fraction adjustment for setup corrections. For IMPT recalculations, bone alignment was carried out to estimate change in the dose distribution after conventional rigid alignment (i.e. 2D-3D patient positioning without fiducials).

The DVH (dose-volume histogram) evaluation was based on QUANTEC organs dose/volume tolerance summary(26).

3. Results

3.1 Contour comparison (Dice coefficient)

A comparison between planning CT and virtual CT contours was carried out. Dice coefficient(33) measurements for PTV and rectum structures are presented in table 1. Automatically generated contours were, in general, adequate for DVH analysis since they followed the organ deformation (figures 4 and 5), requiring minor corrections for smoothing or as required from medical discretion. Patients 2 and 6 presented non full bladder during the planning CT acquisition, resulting in volumes differences up to 90 mL and 120 mL, respectively, compared to virtual CT bladder contours. These results are not intended to validate the DIR, they rather serve as indicator of deforming anatomy.

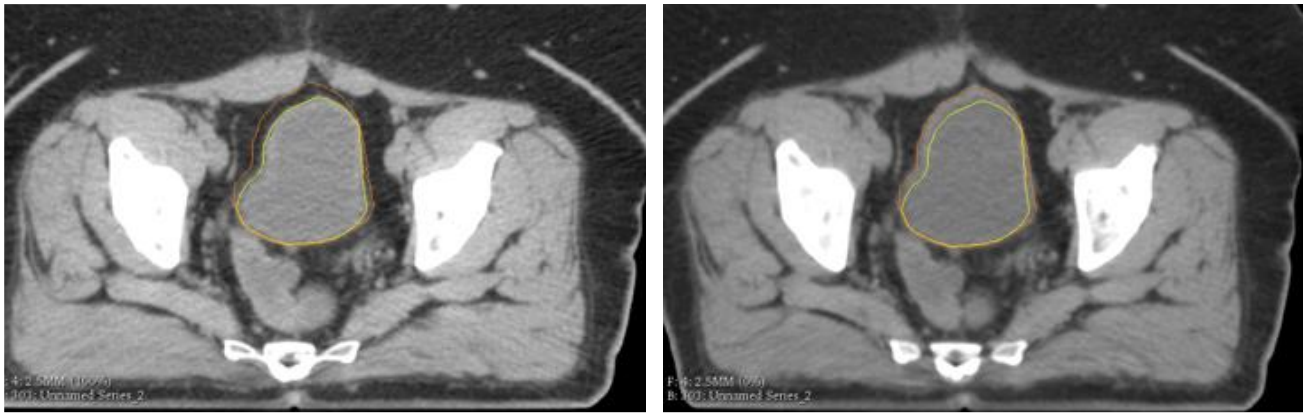

Figure 4: Bladder volume variation from patient's 6 planning CT (left) to $_{v}$CT (right); planning CT contour in yellow and automatically generated contour in orange.

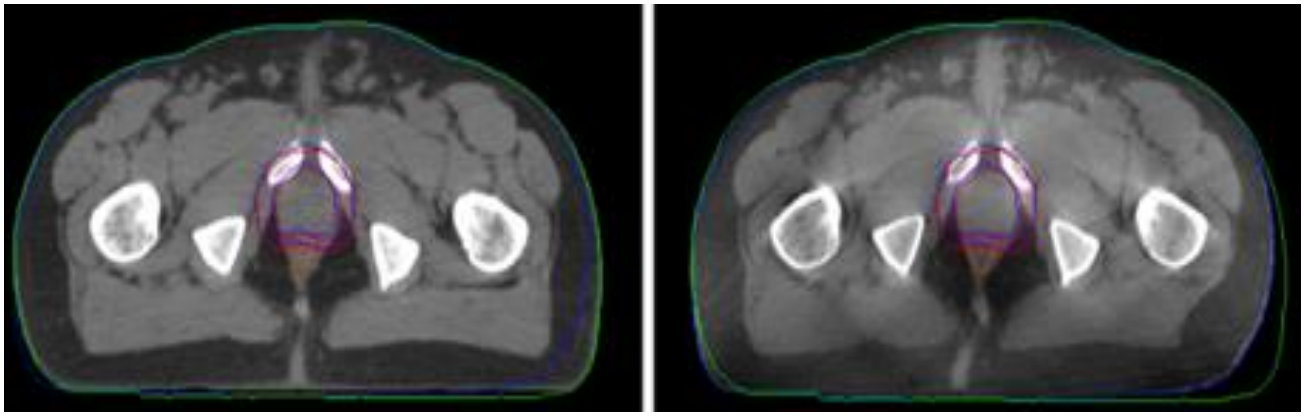

Figure 5: BODY, PTV, CTV and Rectum volumes variation from patient's 1 planning CT (left) to CBCT (right); planning CT contours in green, red and brown. Automatically generated contours in blue and orange.

Table 1: Dice coefficient between planning CT and virtual CT contours.

		CT 1	CT2	CT 3	CT 4
		Dice coeff.	Dice coeff.	Dice coeff.	Dice coeff.
Patient 1	PTV	0.96	0.91	0.99	0.94
	Rectum	0.91	0.92	0.87	0.87
	Bladder	0.96	0.95	0.93	0.94
Patient 2	PTV	0.96	0.96	0.97	0.99
	Rectum	0.89	0.89	0.93	0.94
	Bladder	0.87	0.83	0.93	0.92
Patient 3	PTV	0.95	0.96	0.95	
	Rectum	0.87	0.90	0.89	
	Bladder	0.92	0.94	0.96	
Patient 4	PTV	0.97	0.97	0.97	
	Rectum	0.91	0.93	0.93	
	Bladder	0.97	0.97	0.96	
Patient 5	PTV	0.94	0.95	0.96	
	Rectum	0.84	0.87	0.92	
	Bladder	0.94	0.94	0.92	
Patient 6	PTV	0.95	0.95	0.95	
	Rectum	0.87	0.82	0.82	
	Bladder	0.90	0.86	0.78	
Patient 7	PTV	0.95	0.97	0.97	
	Rectum	0.91	0.88	0.92	
	Bladder	0.95	0.96	0.96	
Patient 8	PTV	0.96	0.97	0.96	
	Rectum	0.88	0.91	0.88	
	Bladder	0.95	0.94	0.91	
Patient 9	PTV	0.97	0.96		
	Rectum	0.93	0.92		
	Bladder	0.94	0.91		

3.2 Deformable image registration validation

Correspondent points between CT and CBCT were identified and their distance calculated for each pair of images. Their distance distribution before and after DIR can be seen in table 2. It can be noticed that, after deformable registration, most of the measured distances lay around the maximum voxel size (2.5 mm), with considerable corrections in comparison with the initial position of landmarks. The applied sign test confirmed a statistically significant reduction of landmark errors following DIR.

3.3 IMRT plan recalculation

For 8 patients, an increase in the rectum dose was observed: for 3 cases the increase was quantified as significant (QUANTEC constraints violation). The extreme case (patient 6) presented approximately V60 = 40%, V70 = 26% and V75 = 19% for rectum. This patient featured an elevated body mass, which implied more difficult position reproducibility and greater anatomical variations between fractions. The PTV presented loss of coverage in some cases, nevertheless the CTV was still receiving the prescribed dose, except for one case where the CTV DVH curve dropped to 75 Gy at 99% of the CTV volume.

3.4 IMPT plan recalculation

The tendencies of DVH modifications for proton therapy plans follow the above-mentioned results for IMRT, regarding dose increase in the rectum. For contralateral proton treatments, patients weight loss and femoral head rotation affected directly the beam range. In figure 6, an example of dose difference between planned and recalculated dose due to weight loss is shown. The local tissue reduction along the beam line path was up to 8 mm. The differences in dose received by the rectum for this case is presented in table 3.

Another noteworthy case presented rectum circumference reduction, resulting in prostate movement in the posterior direction and PTV coverage loss (approx. 63 Gy at 99% of PTV volume). This PTV loss implied also a minimum dose reduction in the CTV from 76 to 71 Gy (less than 95% of the prescribed dose). The DVH analysis for this case is reported in table 4.

Assuming daily image guidance (soft tissue target for photons and bony anatomy for protons), the PTV margin used in this study was still sufficient to assure the prescribed dose delivery to the CTV, except for one patient.

Table 2: Mean distance between landmarks before and after Deformable image registration All distances in mm.

		CT 1		CT 2		CT 3		CT 4	
		Mean	Std	Mean	Std	Mean	Std	Mean	Std
Patient 1	Before	4.23	4.02	5.36	1.23	4.56	3.76	4.60	3.78
	After	2.33	1.30	1.72	1.48	1.69	1.04	2.07	1.18
Patient 2	Before	3.70	4.14	4.13	4.44	3.75	4.29	3.66	3.98
	After	1.87	1.02	1.62	1.02	1.84	1.46	2.09	2.05
Patient 3	Before	3.24	4.65	4.22	4.13	4.57	3.82		
	After	1.51	1.34	1.47	1.22	1.83	1.46		
Patient 4	Before	4.09	4.43	4.15	4.30	4.26	4.54		
	After	1.55	1.57	1.62	1.51	1.73	1.76		
Patient 5	Before	3.13	3.49	3.56	3.92	3.27	3.77		
	After	1.92	1.53	1.53	1.45	3.15	1.39		
Patient 6	Before	3.65	4.07	3.06	3.90	3.75	4.36		
	After	1.58	1.46	1.78	1.60	2.25	0.98		
Patient 7	Before	3.21	2.49	3.34	2.30	2.54	3.48		
	After	1.67	1.37	1.66	1.32	1.82	1.47		
Patient 8	Before	3.91	4.13	4.50	4.25	3.95	3.85		
	After	1.42	0.72	1.68	0.85	2.02	1.29		
Patient 9	Before	2.80	3.28	3.03	3.67				
	After	1.55	1.06	1.64	1.25				

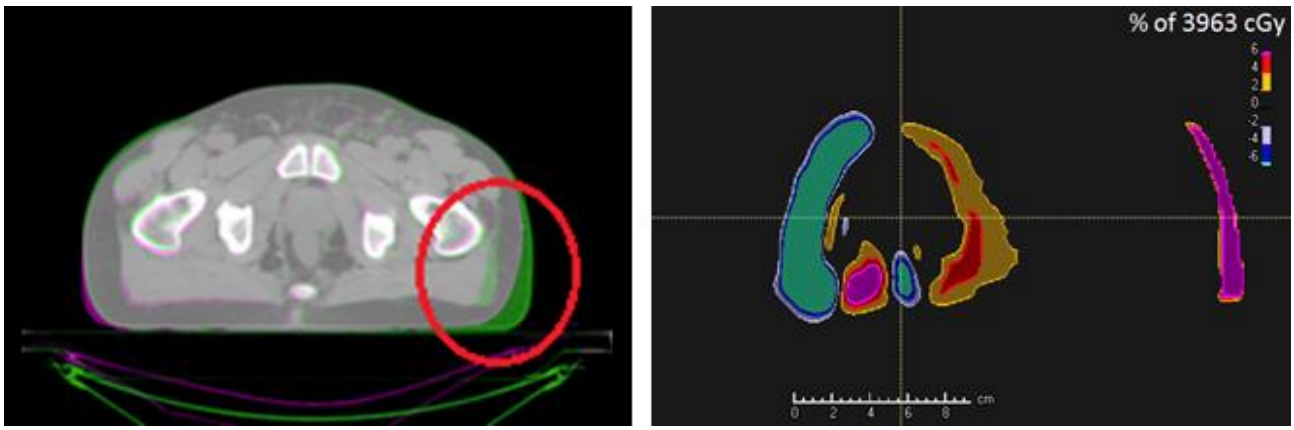

Figure 6: Anatomy difference due to weight loss (left), shown in color overlay. Dose difference after plan recalculation on the correspondent $_{v}$CT.

Table 3: DVH comparison at the rectum for figure 4 case.

	IMRT		IMPT	
	Plan (%)	Recalc (%)	Plan (%)	Recalc (%)
V60	28.1	32.3	25.0	28.2
V65	22.4	27.1	19.9	23.3
V70	16.0	22.7	13.0	17.4
V75	10.3	15.1	4.4	7.0

Table 4: DVH comparison at the rectum for independent prostate motion case.

	IMRT		IMPT	
	Plan (%)	Recalc (%)	Plan (%)	Recalc (%)
V60	27.1	31.2	30.9	19.9
V65	19.3	22.6	20.9	10.8
V70	11.1	14.3	12.7	4.3
V75	3.5	5.1	3.8	0.2

3.5 Dose comparison (gamma test)

Each recalculated dose was compared with its correspondent treatment plan dose. The distance-to-agreement criteria used was 3.00 mm, the dose difference criteria was 3.00 % and the threshold for gamma voxel values calculations was from 10.00 % of the maximum treatment planning dose. These results (table 5) might also represent another form of deformation quantification in the irradiated volume. These results are not intended to validate the DIR, they rather serve as indicator of deforming anatomy and the potential of implementing DIR for adaptive therapy.

4. Discussion

A deformable registration algorithm based on ITK library was developed and tested in 9 prostate cancer cases: the code was validated for CT-CBCT DIR. The automatically propagated contours required small or no corrections, therefore being, at least, a good starting point for fast recontouring the vCT, allowing online DVH verification. The relatively low Dice coefficients found for rectum and bladder structures indicate significant anatomical deformation, which agrees with the large variation highlighted in dose recalculation. When comparing vCT vs. treatment planning CT contours, differences were mostly local, i.e. limited to specific regions. This was also confirmed by Dice coefficient results, which were above 0.78 (Patient 6, bladder contour).

Such results corroborated with the local deformation measurements from landmarks, as reported for deformable image registration validation.

Residual mean errors, measured relying on automatically extracted landmarks, featured the same magnitude as the voxel size, as opposed to initial deformation, exceeding 5 mm on average in worst cases (Table 2). Image resolution is clearly a limiting factor in landmark localization, as landmark distances below 1 voxel cannot be determined. Such a result is optimal at the available image resolution, but it would require further assessment for proton therapy plans, since the 2.5 mm voxel size might be insufficient for accurate planning. Automatic landmark extraction should be therefore applied to higher resolution datasets to achieve adequate confidence on reported results for proton therapy plans.

For both modalities (protons and photons), the rectum is susceptible to structural variations, which may result in early excessive damage of acute-responding component of rectal wall, and might contribute to the initiation of late rectal injury(34,35). Therefore, DIR and dose recalculation are important tools for dose distribution verification in organs at risk, in order to avoid future complications and lesions(19).

For photons, IMRT plans with 5 treatment fields, recalculated on the vCTs, demonstrated robustness for PTV coverage, given the realization of prostate position-based rigid alignment prior to each fraction. Such a results can be achieved relying on daily image guidance with volumetric CBCT, and/or with implanted landmarks/transponders.

For protons, contralateral fields were used, assuming daily image guidance with bony anatomy matching, as currently available in most treatment facilities. Patient anatomical changes on the beam path could result in significant loss of PTV coverage and rectum dose increase, due to proton physical properties. For the studied cases, the used PTV margins were enough to assure the prescribed dose delivery to the CTV, except for one vCT, where prostate motion and femoral head rotation contributed to a significant difference in the dose given to the CTV. This suggests that the availability of CBCT imaging in proton therapy facilities may be beneficial, as this would allow soft tissue imaging in the treatment room.

Yang et al. (36) proposed a method of combining online and offline strategies to address anatomical and weight changes as those verified in our study. This method allows comparable results to online plan adaptation with considerably less effort. Our approach presents vCT as an alternative to in-room CT for this type of plan adaptation, provided that CBCT imaging is available.

Table 5: Dose comparison (Gamma test) between recalculated and planned dose.

	Pass fraction (%) CT 1		**Pass fraction (%) CT 2**		**Pass fraction (%) CT 3**		**Pass fraction (%) CT 4**	
Pat.	Photon	Proton	Photon	Proton	Photon	Proton	Photon	Proton
1	97.31	97.52	94.45	93.70	97.23	80.70	93.00	86.67
2	98.33	92.32	93.05	92.93	96.31	93.06	90.76	99.40
3	96.53	94.00	97.13	96.08	97.25	81.90		
4	98.69	94.90	98.36	96.23	98.11	97.93		
5	92.66	94.13	92.92	94.06	93.76	94.06		
6	95.06	94.08	95.94	86.94	97.92	96.05		
7	96.59	90.37	92.83	95.38	97.89	91.40		
8	94.97	96.96	93.75	94.53	97.35	90.95		
9	94.88	96.28	97.08	94.78				

Kurz et al. demonstrated the use of vCT as a prior for scatter correction in CBCT and showed that DIR generated contours from vCT might not be accurate. Our results benefited from high quality CBCT images, allowing DIR generated contours to serve as initial guess of new anatomy recontouring, despite more pronounced anatomy changes when compared to H&N cases.

This study describes an analysis on anatomy variation with a limited number of CBCT per patient (up to 4) during the treatment. We suggest a methodology that uses DIR as a tool to evaluate if the anatomical changes would result in insufficient dose distribution, regarding the treatment planning. Therefore, if significant changes are found, it might point to a necessity for re-planning.

Future studies with daily CBCT would allow daily anatomical changes tracking, dose of the day calculation and later dose accumulation, which could be related to acute effects of radiation. Providing relevant information for future IGRT guidelines.

5. Conclusions

Both modalities presented increased rectum dose in 8 of 9 patients, resulting in QUANTEC constraints violation for 3 cases. CTV reduced coverage is more likely to happen for IMPT when the patient is positioned relying on bone anatomy. Our results point out the potential of using CBCT and DIR to account for anatomical changes for IMRT and IMPT prostate patients, despite limitations of CBCT imaging in the pelvic region.

Acknowledgment

The author was supported in part by the Coordination for the Improvement of Higher Education Personnel (CAPES) - Grant 9374-13-2.

References

1. Tuohy R, Bosse C, Mavroidis P, Shi Z, Crownover R, Papanikolaou N, et al. Deformable image and dose registration evaluation using two commercial programs. Int J Cancer Ther Oncol. 2014;2(2).
2. Lou Y, Niu T, Jia X, Vela P a., Zhu L, Tannenbaum AR. Joint CT/CBCT deformable registration and CBCT enhancement for cancer radiotherapy. Med Image Anal [Internet]. 2013;17(3):387–400. Available from: http://dx.doi.org/10.1016/j.media.2013.01.005
3. Ghilezan M, Yan D, Martinez A. Adaptive Radiation Therapy for Prostate Cancer. Semin Radiat Oncol. 2013;20(2):130–7.
4. Estro 33, 2014. :1682.
5. Veiga C, Janssens G, Teng CL, Baudier T, Hotoiu L, McClelland JR, et al. First Clinical Investigation of Cone Beam Computed Tomography and Deformable Registration for Adaptive Proton Therapy for Lung Cancer. Int J Radiat Oncol Biol Phys [Internet]. 2016 [cited 2017 Jun 5];95(1):549–59. Available from: http://www.sciencedirect.com/science/article/pii/S0360301616001085
6. Veiga C, Alshaikhi J, Amos R, Lourenço AM, Modat M, Ourselin S, et al. Cone-Beam Computed Tomography and Deformable Registration-Based "Dose of the Day" Calculations for Adaptive Proton Therapy. Int J Part Ther [Internet]. 2015;2(2):150827080102009. Available from: http://theijpt.org/doi/10.14338/IJPT-14-00024.1
7. Veiga C, Alshaikhi J, Amos R. Cone-Beam Computed Tomography and Deformable Registration-Based '" Dose of the Day "' Calculations for Adaptive Proton Therapy. Int J Part Ther. 2015;2(2):1–11.
8. Landry G, Nijhuis R, Dedes G, Handrack J, Thieke C, Janssens G, et al. Investigating CT to CBCT image registration for head and neck proton therapy as a tool for daily dose recalculation. Med Phys [Internet]. 2015;42(3):1354–66. Available from: http://scitation.aip.org/content/aapm/journal/medphys/42/3/10.1118/1.4908223
9. Foley D, McClean B, McBride P. Adaptation of daily dose using CBCT imaging. Phys Medica [Internet]. 2016 Jul [cited 2017 Jun 20];32(7):950. Available from: http://linkinghub.elsevier.com/retrieve/pii/S1120179716300552
10. Hinault P, Compagnon F, Lacaze T, Bachaud JM, Graulieres E. 6. Adaptive radiotherapy: Evaluation of the dose actually delivered to the patient in a treatment of prostate cancer radiotherapy. Phys Medica [Internet]. 2016;32:344. Available from: http://linkinghub.elsevier.com/retrieve/pii/S1120179716310341
11. Kozak KR, Kachnic L a., Adams J, Crowley EM, Alexander BM, Mamon HJ, et al. Dosimetric Feasibility of Hypofractionated Proton Radiotherapy for Neoadjuvant Pancreatic Cancer Treatment. Int J Radiat Oncol Biol Phys. 2007;68(5):1557–66.
12. Rombi B, Delaney TF, MacDonald SM, Huang MS, Ebb DH, Liebsch NJ, et al. Proton radiotherapy for pediatric Ewing's sarcoma: Initial clinical outcomes. Int J Radiat Oncol Biol Phys. 2012;82(3):1142–8.
13. Nichols RC, Huh SN, Prado KL, Yi BY, Sharma NK, Ho MW, et al. Protons offer reduced normal-tissue exposure for patients receiving postoperative radiotherapy for resected pancreatic head cancer. Int J Radiat Oncol Biol Phys [Internet]. 2012;83(1):158–63. Available from: http://dx.doi.org/10.1016/j.ijrobp.2011.05.045
14. Flejmer AM, Nyström PW, Dohlmar F, Josefsson D, Dasu A. Potential Benefit of Scanned Proton Beam versus Photons as Adjuvant Radiation Therapy in Breast Cancer. Int J Part Ther [Internet]. 2015;1(4):845–55. Available from: http://theijpt.org/doi/10.14338/IJPT-14-00013.1
15. Slater JM, Ling TC, Mifflin R, Nookala P, Grove R, Ly AM, et al. Protons Offer Reduced Tissue Exposure for Patients Receiving Radiation Therapy for Pancreatic Cancer. Int J Part Ther [Internet]. 2014;1(3):702–10. Available from: http://theijpt.org/doi/abs/10.14338/IJPT-14-00008.1
16. Lomax AJ. Myths and realities of range uncertainty. Br J Radiol. 2019;20190582.
17. Haverkort M a D, Van De Kamer JB, Pieters BR, Van Tienhoven G, Assendelft E, Lensing AL, et al. Position verification for the prostate: Effect on rectal wall dose. Int J Radiat Oncol Biol Phys. 2011;80(2):462–8.
18. Litzenberg DW, Balter JM, Hadley SW, Sandler HM, Willoughby TR, Kupelian P a., et al. Influence of intrafraction motion on margins for prostate radiotherapy. Int J Radiat Oncol Biol Phys. 2006;65(2):548–53.
19. Scaife J, Harrison K, Romanchikova M, Parker A, Sutcliffe M, Bond S, et al. Random variation in rectal position during radiotherapy for prostate cancer is two to three times greater than that predicted from prostate motion. Br J Radiol. 2014;87(1042).
20. Akino Y, Yoshioka Y, Fukuda S, Maruoka S, Takahashi Y, Yagi M, et al. Estimation of rectal dose using daily megavoltage cone-beam computed tomography and deformable image registration. Int J Radiat Oncol Biol Phys. 2013;87(3):602–8.
21. Desplanques M, Tagaste B, Fontana G, Pella A, Riboldi M, Fattori G, et al. A comparative study between the imaging system and the optical tracking system in proton therapy at CNAO. J Radiat Res. 2013;54.
22. Johnson HJ, Mccormick M, Ibanez L, Consortium IS. The ITK Software Guide Third Edition - Updated for ITK version 4.5 [Internet]. 2013. Available from: http://itk.org/ItkSoftwareGuide.pdf
23. Pugh TJ, Munsell MF, Choi S, Nguyen QN, Mathai B, Zhu XR, et al. Quality of life and toxicity from passively scattered and spot-scanning proton beam therapy for localized prostate cancer. Int J Radiat Oncol Biol Phys

[Internet]. 2013;87(5):946–53. Available from: http://dx.doi.org/10.1016/j.ijrobp.2013.08.032
24. Mendenhall NP, Hoppe BS, Nichols RC, Mendenhall WM, Morris CG, Li Z, et al. Five-year outcomes from 3 prospective trials of image-guided proton therapy for prostate cancer. Int J Radiat Oncol Biol Phys [Internet]. 2014;88(3):596–602. Available from: http://dx.doi.org/10.1016/j.ijrobp.2013.11.007
25. Ferjani S, Huang G, Shang Q, Stephans KL, Zhong Y, Qi P, et al. Alignment focus of daily image guidance for concurrent treatment of prostate and pelvic lymph nodes. Int J Radiat Oncol Biol Phys [Internet]. 2013;87(2):383–9. Available from: http://dx.doi.org/10.1016/j.ijrobp.2013.06.003
26. Marks LB, Yorke ED, Jackson A, Ten Haken RK, Constine LS, Eisbruch A, et al. Use of Normal Tissue Complication Probability Models in the Clinic. Int J Radiat Oncol Biol Phys [Internet]. 2010 Mar 1 [cited 2017 Jul 8];76(3 SUPPL.):S10-9. Available from: http://linkinghub.elsevier.com/retrieve/pii/S036030160903288X
27. Lowe DG. Distinctive Image Features from Scale-Invariant Keypoints. Int J Comput Vis. 2004;60(2):91–110.
28. Cheung W, Hamarneh G. n-SIFT: n-Dimensional scale invariant feature transform. IEEE Trans Image Process. 2009;18(9):2012–21.
29. Paganelli C, Peroni M, Riboldi M, Sharp GC, Ciardo D, Alterio D, et al. Scale invariant feature transform in adaptive radiation therapy: a tool for deformable image registration assessment and re-planning indication. Phys Med Biol [Internet]. 2013;58:287–99. Available from: http://www.ncbi.nlm.nih.gov/pubmed/23257263
30. Mattes D, Haynor D. Nonrigid multimodality image registration. In: SPIE [Internet]. 2001. p. 1609–20. Available from: http://dx.doi.org/10.1117/12.431046%5Cnhttp://proceedings.spiedigitallibrary.org/data/Conferences/SPIEP/35163/1609_1.pdf
31. Zhu Q, Gu J, Xie Y. Deformable Image Registration with Inclusion of Autodetected Homologous Tissue Features. Sci World J [Internet]. 2012;2012:1–8. Available from: http://www.hindawi.com/journals/tswj/2012/913693/
32. Shackleford J a, Shusharina N, Verberg J, Winey B, Neuner M, Steininger P, et al. Plastimatch 1 . 6 – Current Capabilities and Future Directions. 2012;(January).
33. Zou KH, Warfield SK, Bharatha A, Tempany CMC, Kaus MR, Haker SJ, et al. Statistical Validation of Image Segmentation Quality Based on a Spatial Overlap Index. Acad Radiol [Internet]. 2004 [cited 2020 Jul 10];11(2):178–89. Available from: /pmc/articles/PMC1415224/?report=abstract
34. Wang C-JJ, Leung SW, Chen H-CC, Sun L-MM, Fang F-MM, Huang E-YY, et al. The correlation of acute toxicity and late rectal injury in radiotherapy for cervical carcinoma: Evidence suggestive of consequential late effect (CQLE). Int J Radiat Oncol Biol Phys [Internet]. 1998 Jan 1 [cited 2017 Jun 5];40(1):85–91. Available from: http://www.sciencedirect.com/science/article/pii/S0360301697005609
35. Michalski JM, Gay H, Jackson A, Tucker SL, Deasy JO. Radiation Dose–Volume Effects in Radiation-Induced Rectal Injury. Int J Radiat Oncol [Internet]. 2010 [cited 2017 Jun 5];76(3):S123–9. Available from: http://www.sciencedirect.com/science/article/pii/S036030160903291X
36. Yang C, Liu F, Ahunbay E, Chang YW, Lawton C, Schultz C, et al. Combined online and offline adaptive radiation therapy: A dosimetric feasibility study. Pract Radiat Oncol [Internet]. 2014;4(1):e75–83. Available from: http://dx.doi.org/10.1016/j.prro.2013.02.012

Contato:

Roberto Cassetta
Varian Medical Systems
Taefernstrasse 7, Daettwil 5405 Switzerland
roberto.cassetta@varian.com